Real-time scattering in Ising field theory using matrix product states

Raghav Jha, Ash Milsted, Dominik Neuenfeld, John Preskill, Pedro Vieira




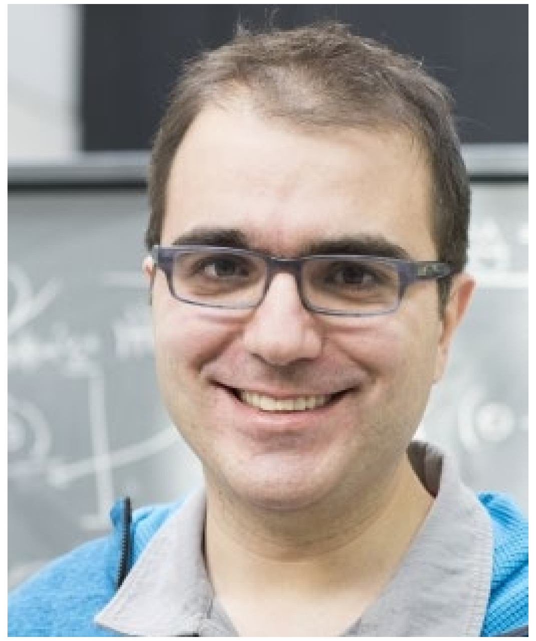

arXiv:2411.13645

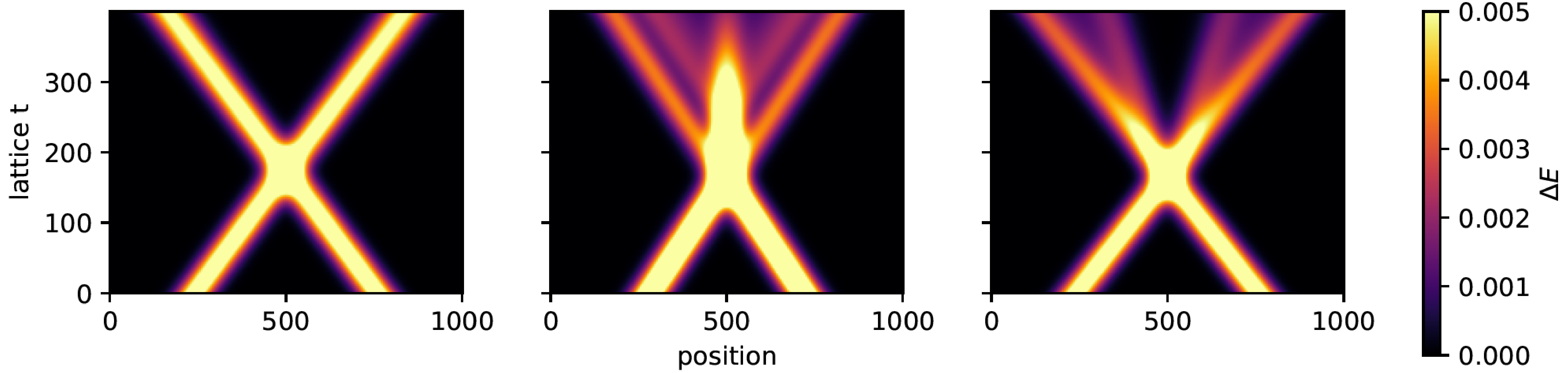

elastic resonance inelastic

Quantum simulation of quantum field theory

50 years since Ken Wilson proposed lattice gauge theory!

Real-time evolution (collider physics), nonzero chemical potential (early universe, neutron stars), …

What's classically hard? Processes that produce highly entangled states, e.g., multiparticle production, quench, …

Laying the foundations for more revealing future work.

Stepping stone to quantum gravity.

New concepts and insights?

Milsted, Liu, Preskill, Vidal

Collisions of false-vacuum bubble walls in a quantum spin chain

PRX Quantum 2022

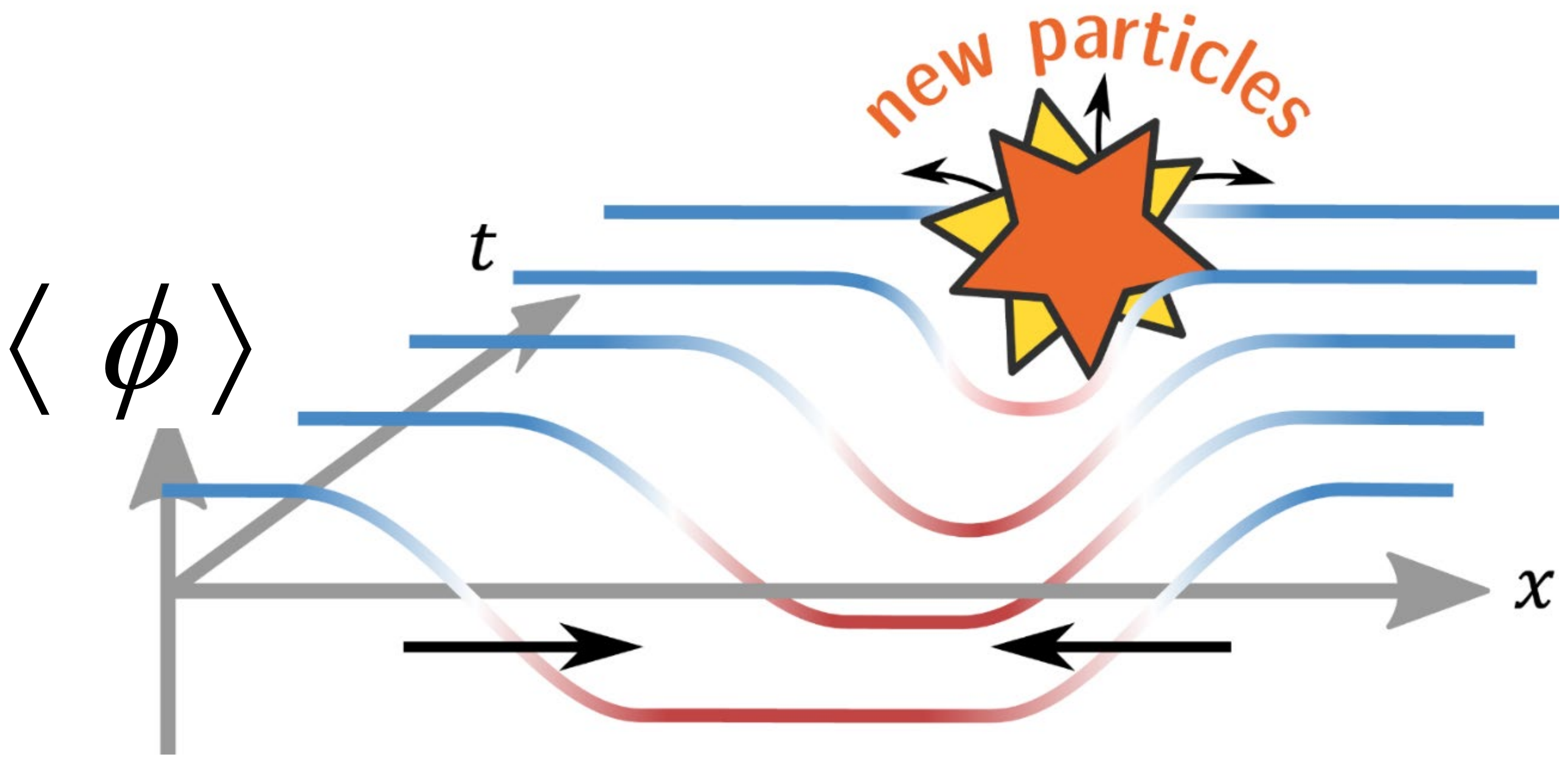

Kink-antikink scattering: Lots of entropy generated, so hard to simulate classically.

Excitations are nonperturbative (cf. proton in large-*N* QCD). A baby version of what we'll need in QCD.

And it's not obvious what happens at strong coupling.

Emergent field theory in a spin system. Heuristic, but more likely to be feasible using near-term platforms. And interesting in its own right. (Cf. colliding bubble walls in the early universe.)

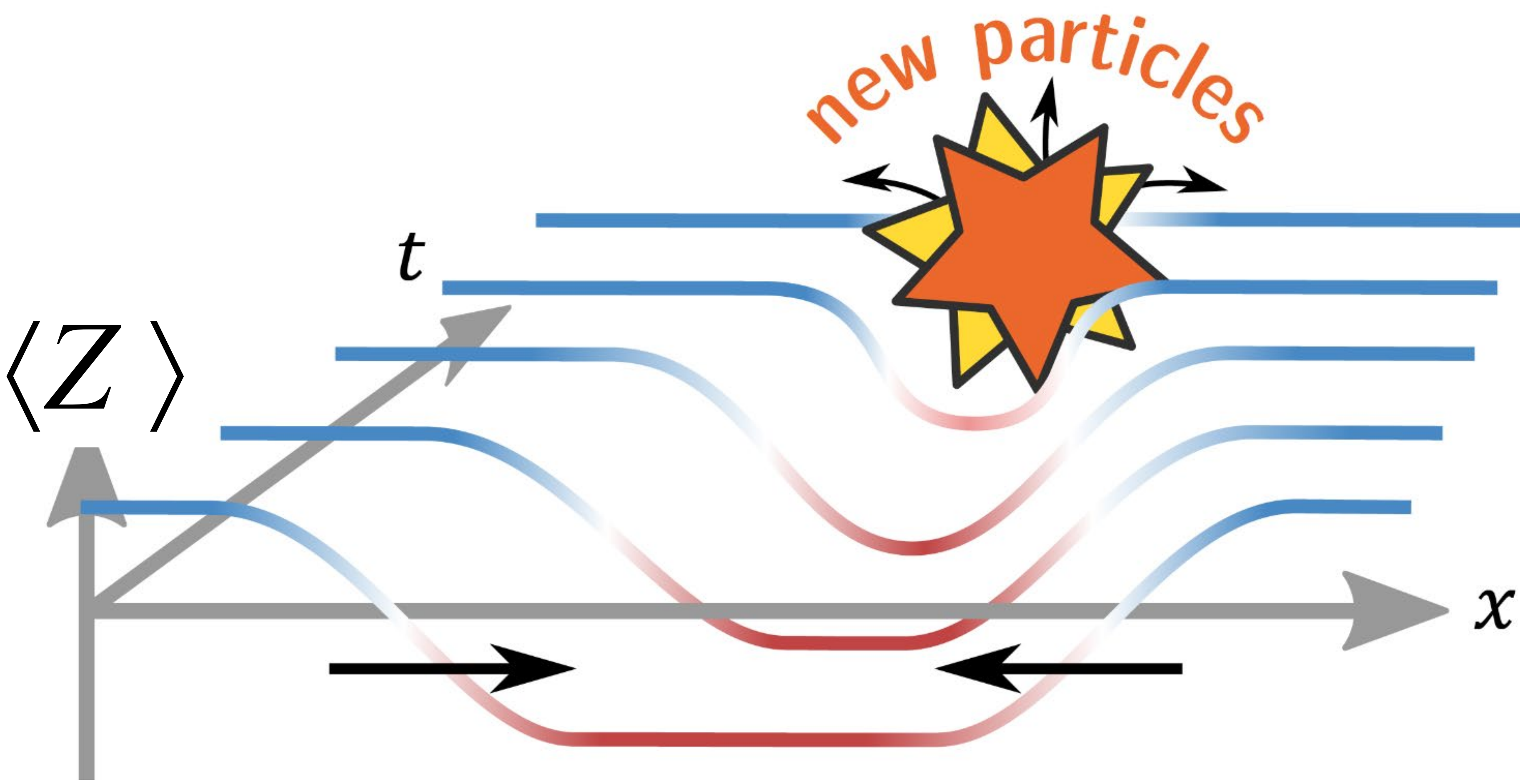

Explicit symmetry breaking (false vacuum)

$$H=\sum_{j=1}^{N}\left[-Z_jZ_{j+1}-gX_j-hZ_j+\lambda\left(X_jZ_{j+1}Z_{j+2}+Z_jZ_{j+1}X_{j+2}\right)\right]$$

We want a spin chain with these features:

-- Emergent Lorentz-invariant field theory
-- Spontaneously broken discrete symmetry
-- Not integrable (or too close to integrable)

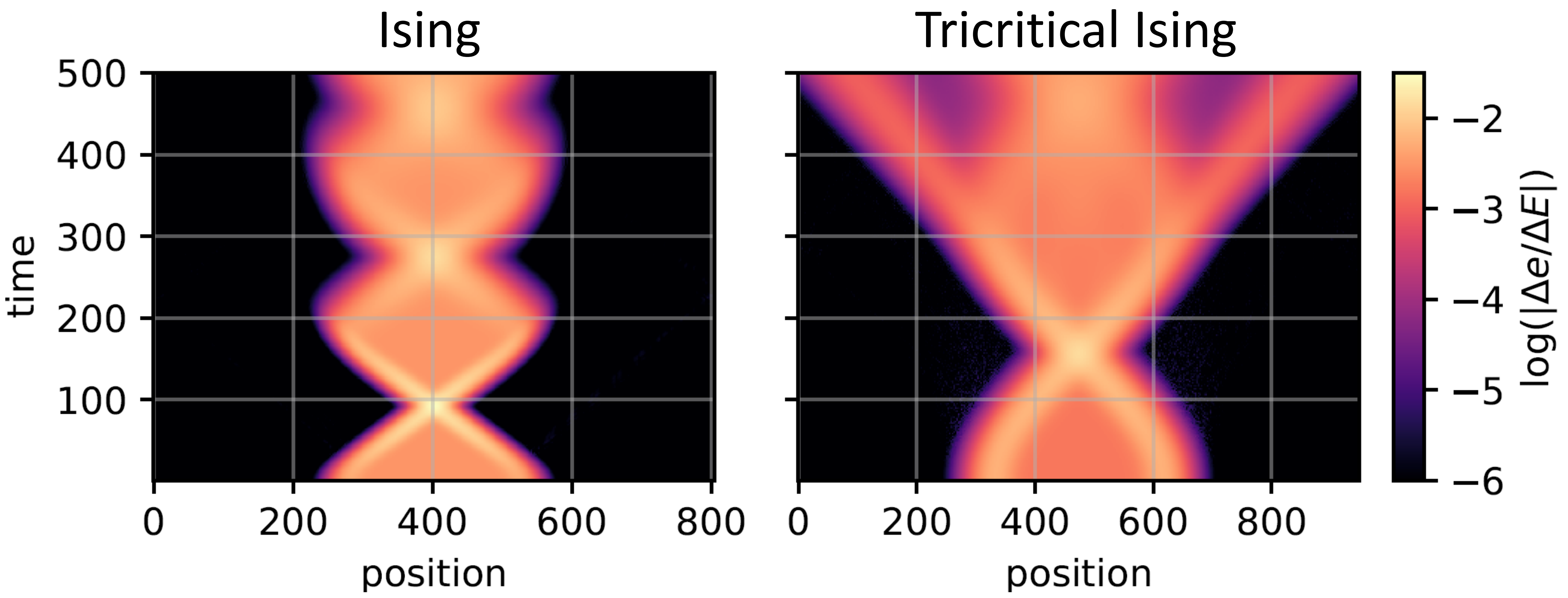

Here excess energy density (relative to the true vacuum) is plotted as a function of position and time.

A kink-antikink pair with false vacuum in between is confined. They collide repeatedly.

The IR limit of the Ising model with $Z2$ symmetry broken ($\lambda = 0$) is an integrable theory. Kinks "bounce" --- no new particles are produced.

The tricritical Ising model ($\lambda \neq 0$) is a nonintegrable field theory. Unconfined "mesons" are produced which propagate ballistically.

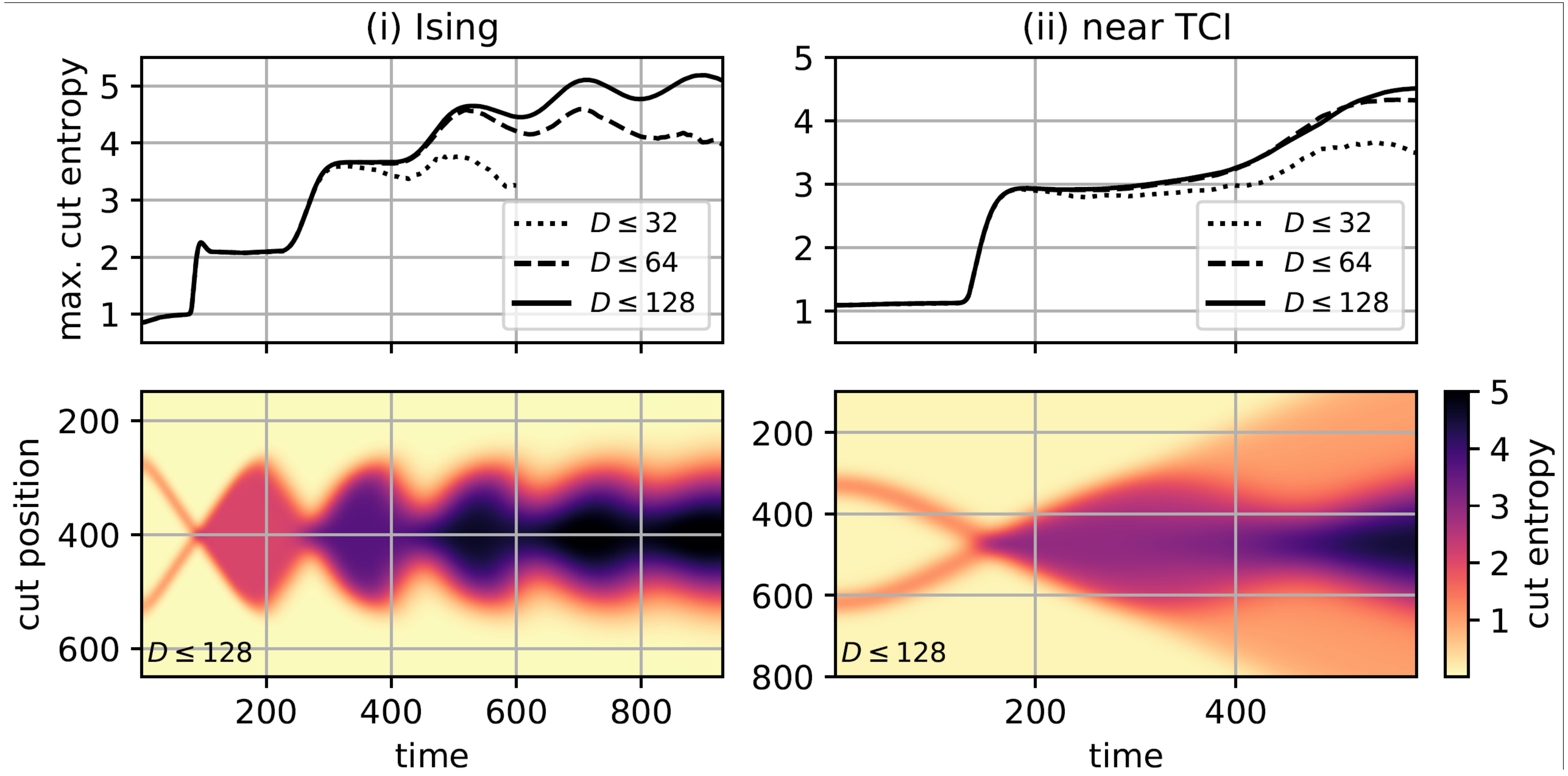

Here entanglement entropy across a cut is plotted as a function of time.

Entropy can increase due to either elastic scattering of wave packets (momentum dependence of scattering phase shift), or due to inelastic particle production.

As entropy increases, a larger bond dimension *D* is needed to approximate the state accurately.

Ising field theory: A line of nonintegrable theories connecting free fermions and E_8

$$I_{\rm IFT} = I_{\rm ICFT} - \tau \int d^2x\,\epsilon(x) - h\int d^2x\,\sigma(x), \quad \eta \equiv \frac{\tau}{|h|^{8/15}}$$

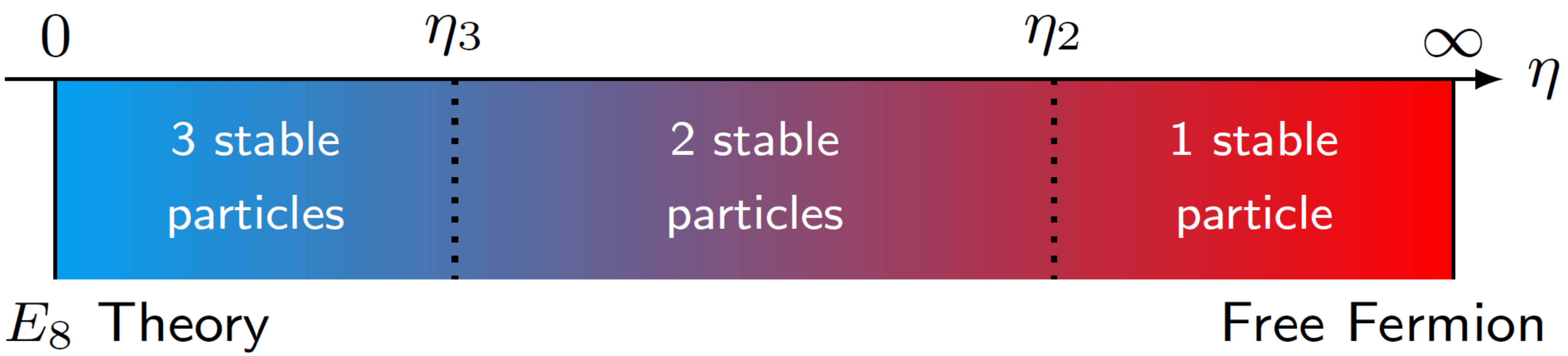

$$H = -\sum_{j=0}^{N}\left(\sigma_j^z\sigma_{j+1}^z + g_x\sigma_j^x + g_z\sigma_j^z\right), \qquad \eta_{\rm latt} = \frac{g_x - 1}{|g_z|^{8/15}}$$

MPS representation of incoming wave packets

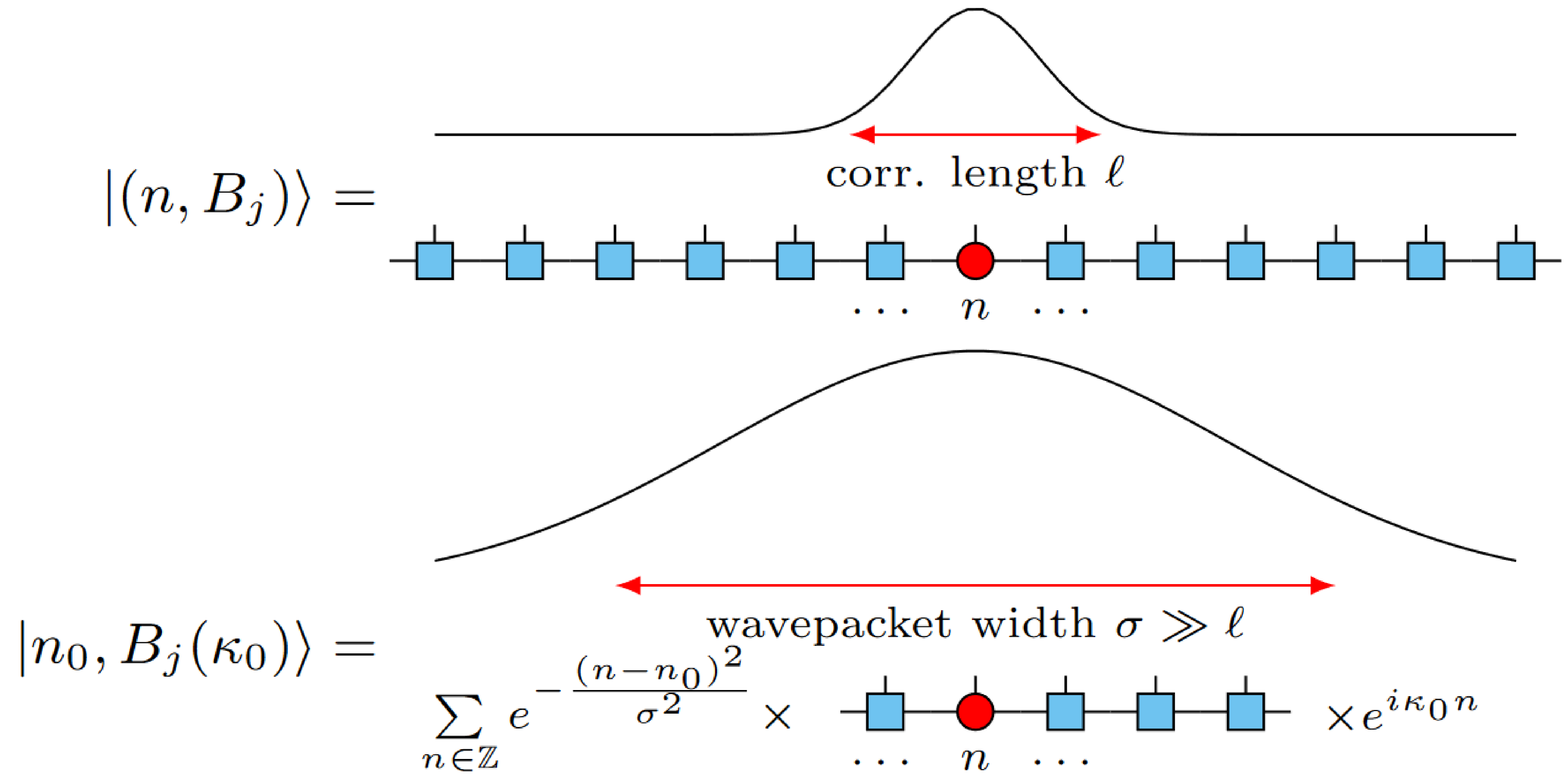

Blue square = “vacuum tensor.” Red circle = “excitation tensor.”

Excitation tensor at a specified site affects the wavefunction in a region with size comparable to correlation length.

Wave packets are spatially broad compared to the correlation length.

1000-2000 sites, bond dimension 64, correlation length 4-10 sites, wavepacket width 70-100 sites.

Scattering outcomes in superposition and energy-density correlators

We see tracks for 11 → 11, 12, 21 (22 kinematically excluded).

Larger η_{latt}: tracks for 11 → 11, 111.

Two-body state. Specifying position of left-mover determines position of right-mover.

Three-body state. Specifying position of leftmost and rightmost particles determines position of middle particle.

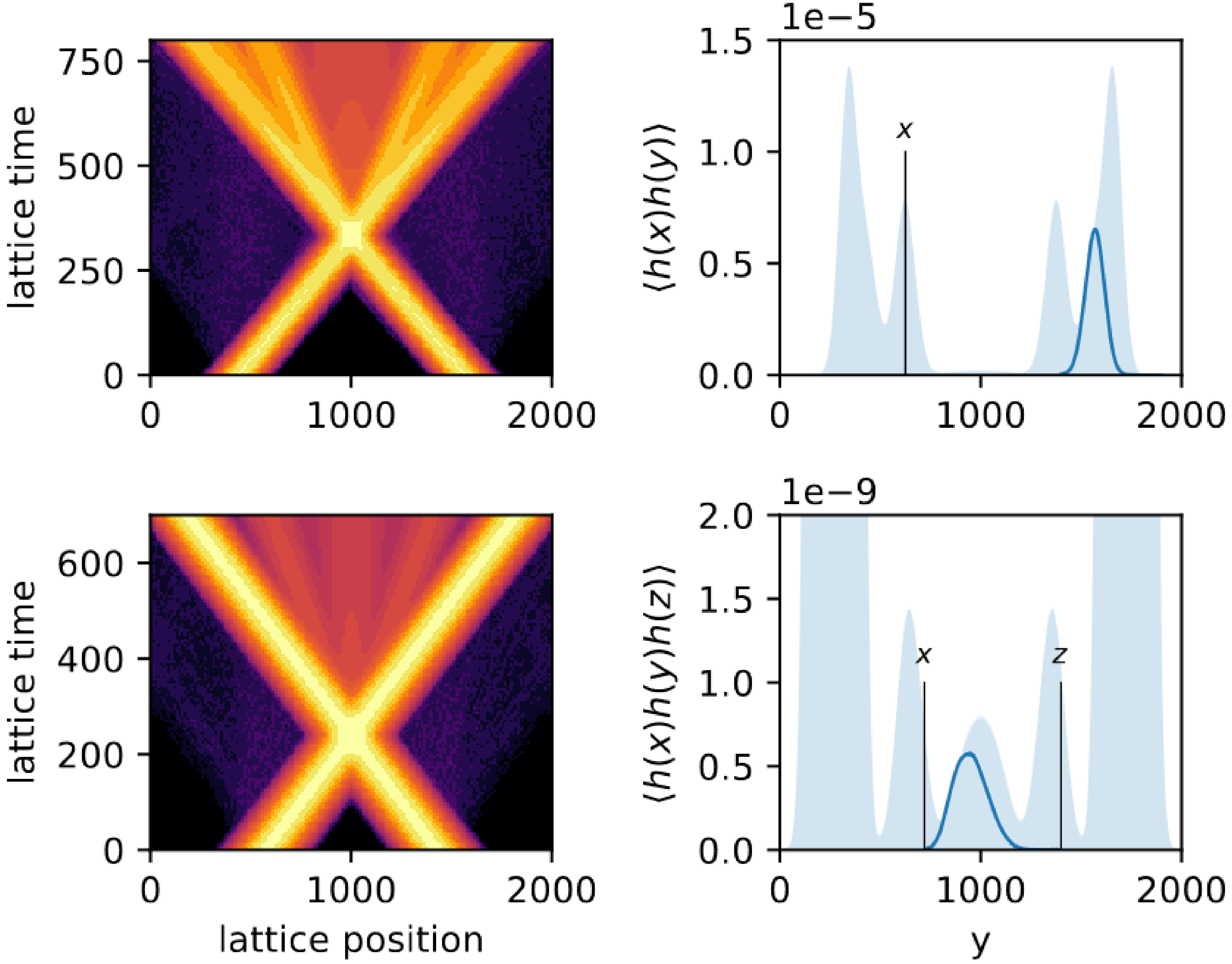

Particle production close to free-fermion theory

$$S_{11\to11}^{\mathrm{nFF}}(\theta) \simeq -\frac{\sinh\theta + i\sin\frac{\pi}{3}}{\sinh\theta - i\sin\frac{\pi}{3}} \times \frac{\sinh\theta - i\sin(\frac{\pi}{3}-\varepsilon)}{\sinh\theta + i\sin(\frac{\pi}{3}-\varepsilon)} \simeq \frac{i\varepsilon}{\theta - 2\pi i/3} + \ldots$$

(CDD factors) $\quad \varepsilon \propto \xi^2, \quad \xi = \eta^{-15/8} = \dfrac{|h|}{\tau^{15/8}}.$

One-parameter fit to probability of 11→111 (Zamolodchikov and Ziyatdinov 2011) determines the relation between lattice and continuum values of ξ.

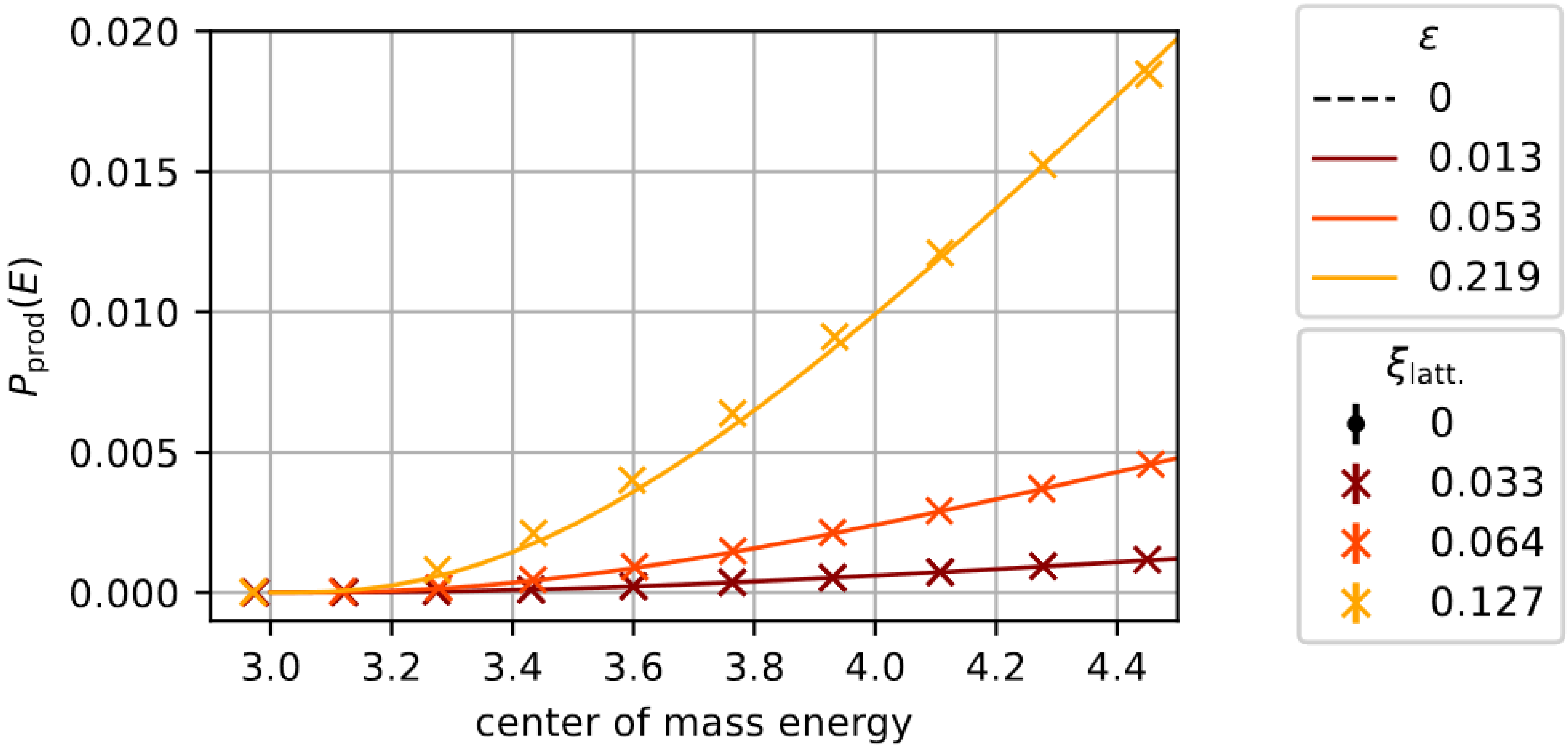

Time delay close to free-fermion theory

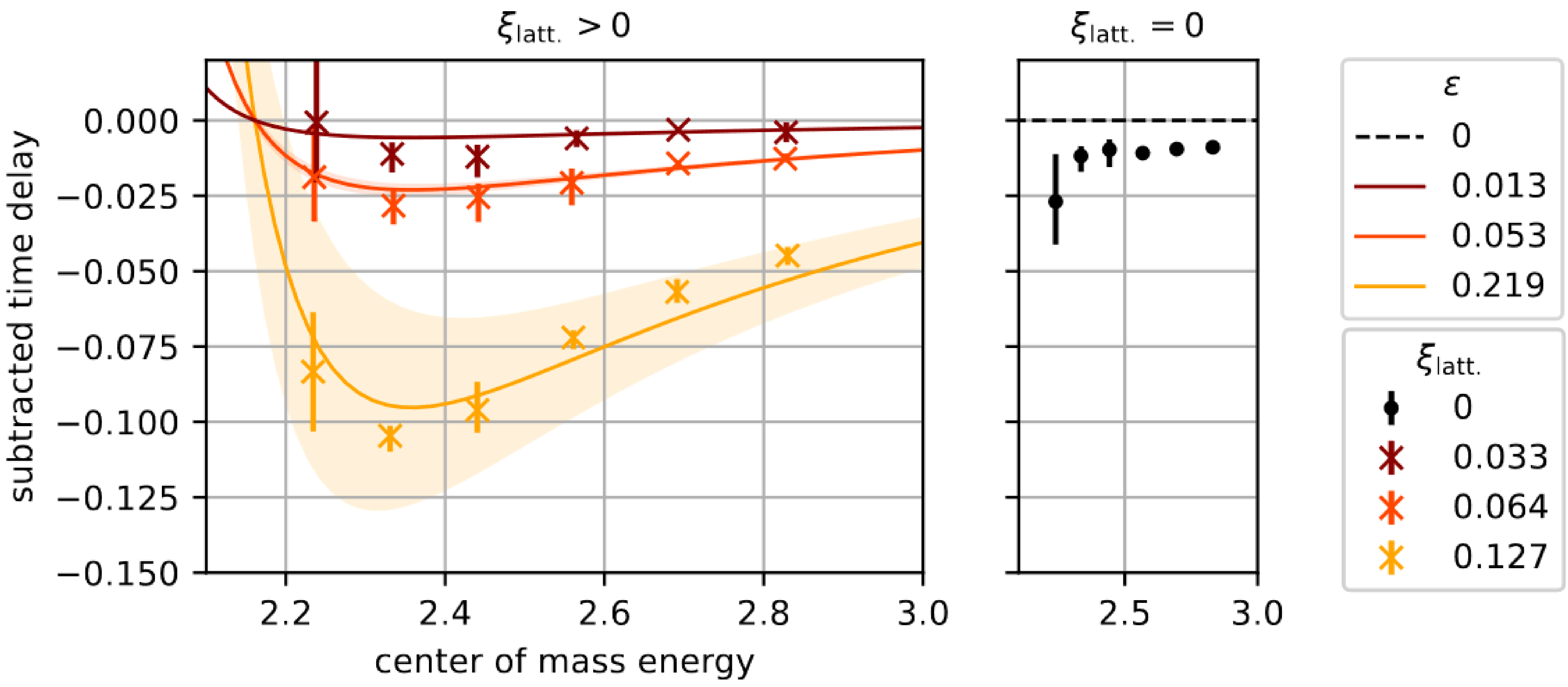

Reasonable agreement with perturbation theory. (Shading shows estimated next-order in ξ correction.)

Close to E_8: enhanced particle production near two-particle thresholds

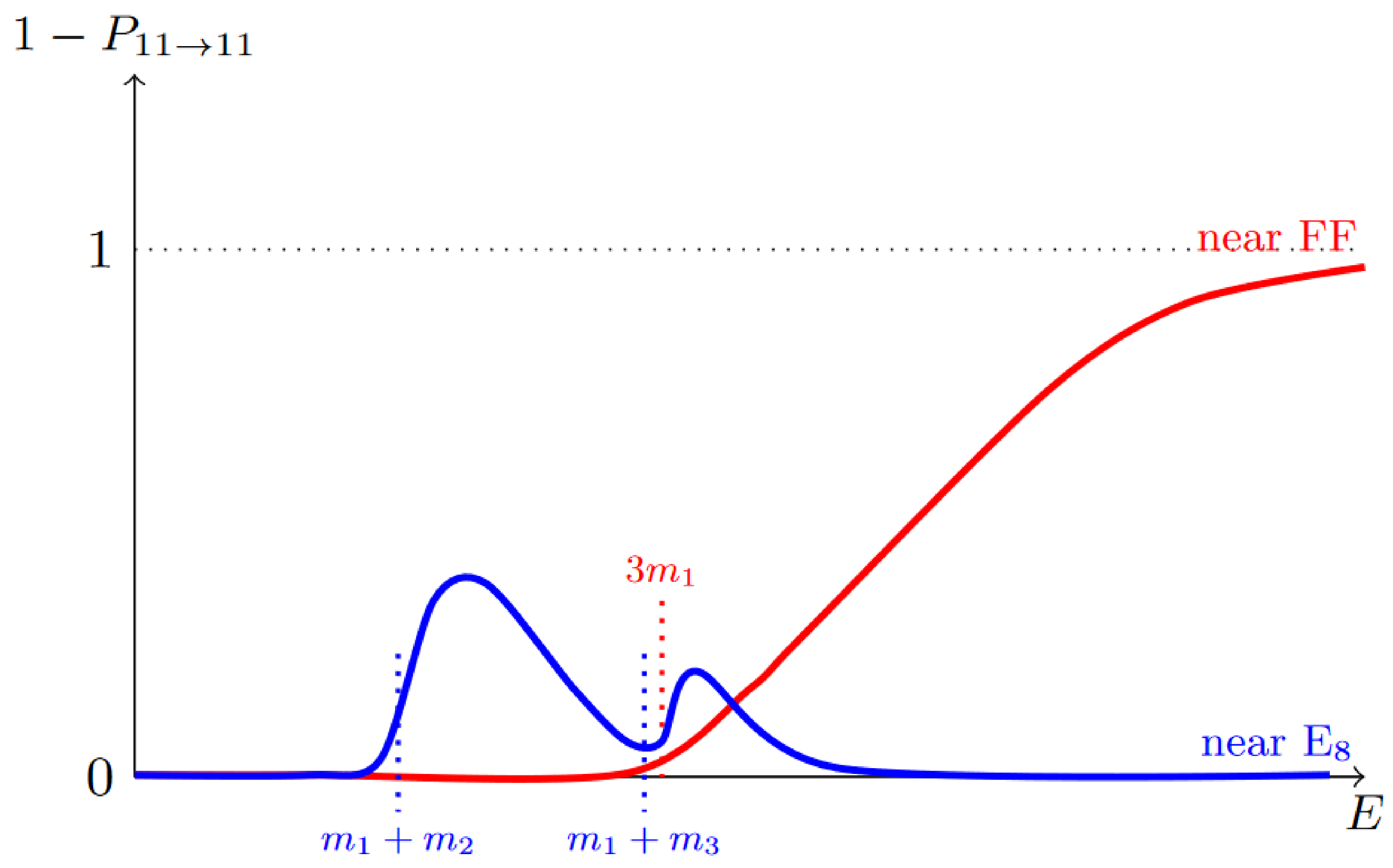

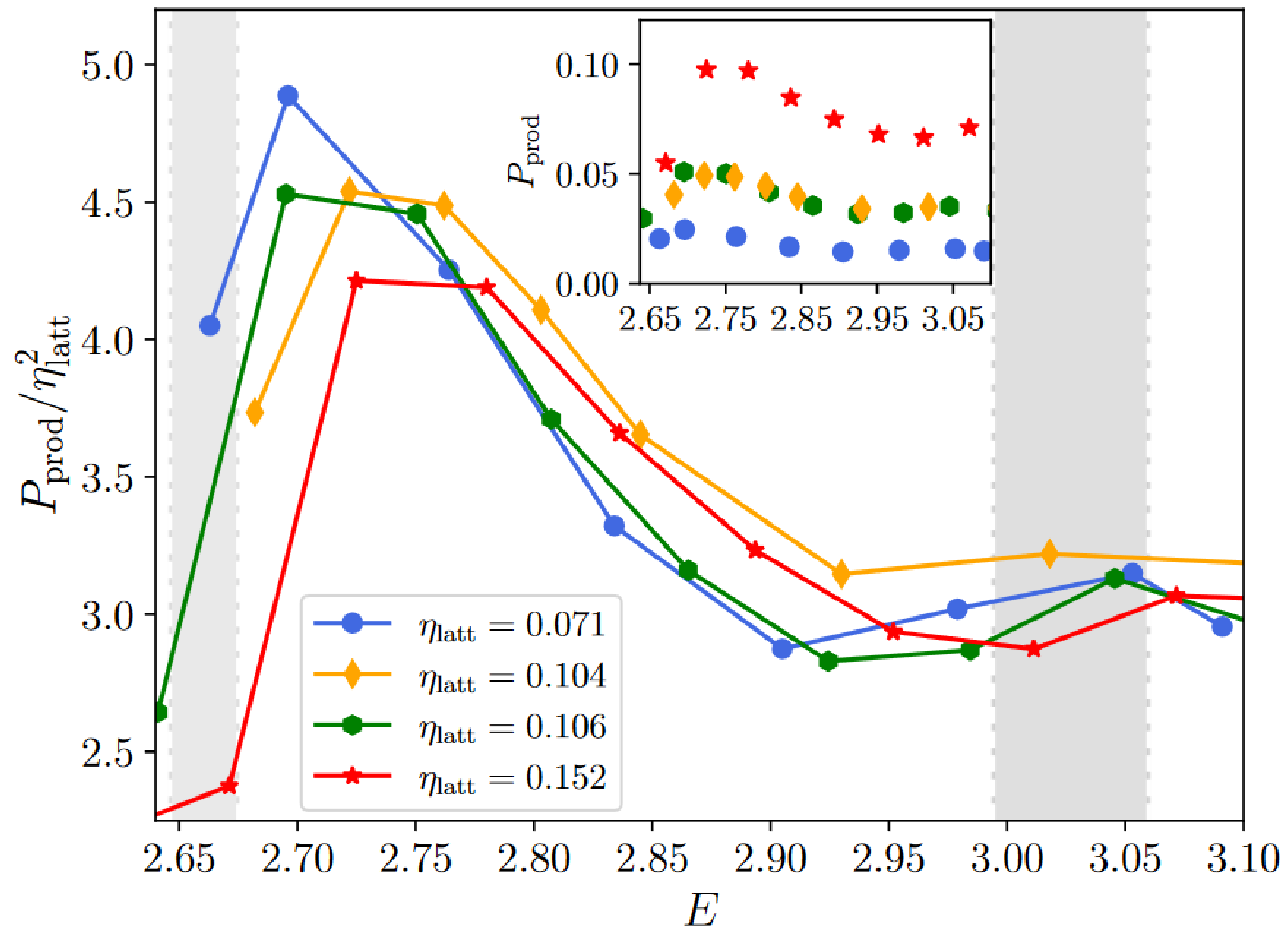

Close to E_8, the probability of inelastic particle production is enhanced where new two-particle channels open up (e.g., 12 and 13), then (per Zamolodchikov 2013) decays as the energy continues to increase.

Close to E_8: resonance peak in the elastic scattering time delay

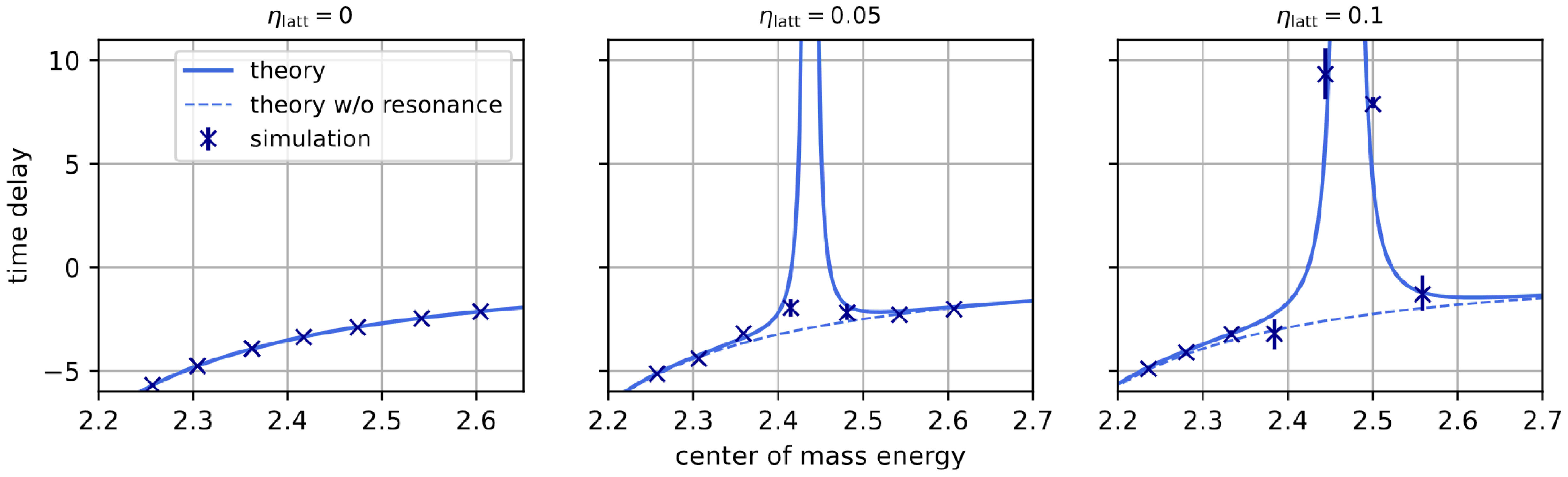

$$\mathrm{Re}(m_4) = 2.404 + 2.33\eta + \mathcal{O}(\eta^2),$$

$$\mathrm{Im}(m_4) = -3.71\eta^2 + \mathcal{O}(\eta^3).$$

(Delfino, Grinza, Mussardo 2006)

$$S^{E_8}{}_{11\to 11}(\theta) = \ldots \times \frac{\sinh\theta + i\sin\alpha_j}{\sinh\theta - i\sin\alpha_j} \times \frac{\sinh\theta + i\sin\alpha_j^*}{\sinh\theta - i\sin\alpha_j^*}.$$

$\eta \simeq (0.28)\eta_{\rm latt}$ from particle spectrum.

Robust estimate of the resonance width

Compute projection onto outgoing particles in the 11 sector.

The probability of not being in the 11 sector decays exponentially in time at a rate determined by the resonance width.

Excess energy (above vacuum) in a central spatial window decays at the same rate.

The spacing of the double tracks depends (predominantly) on the wave-packet width. It arises from destructive interference between resonant and non-resonant contributions.

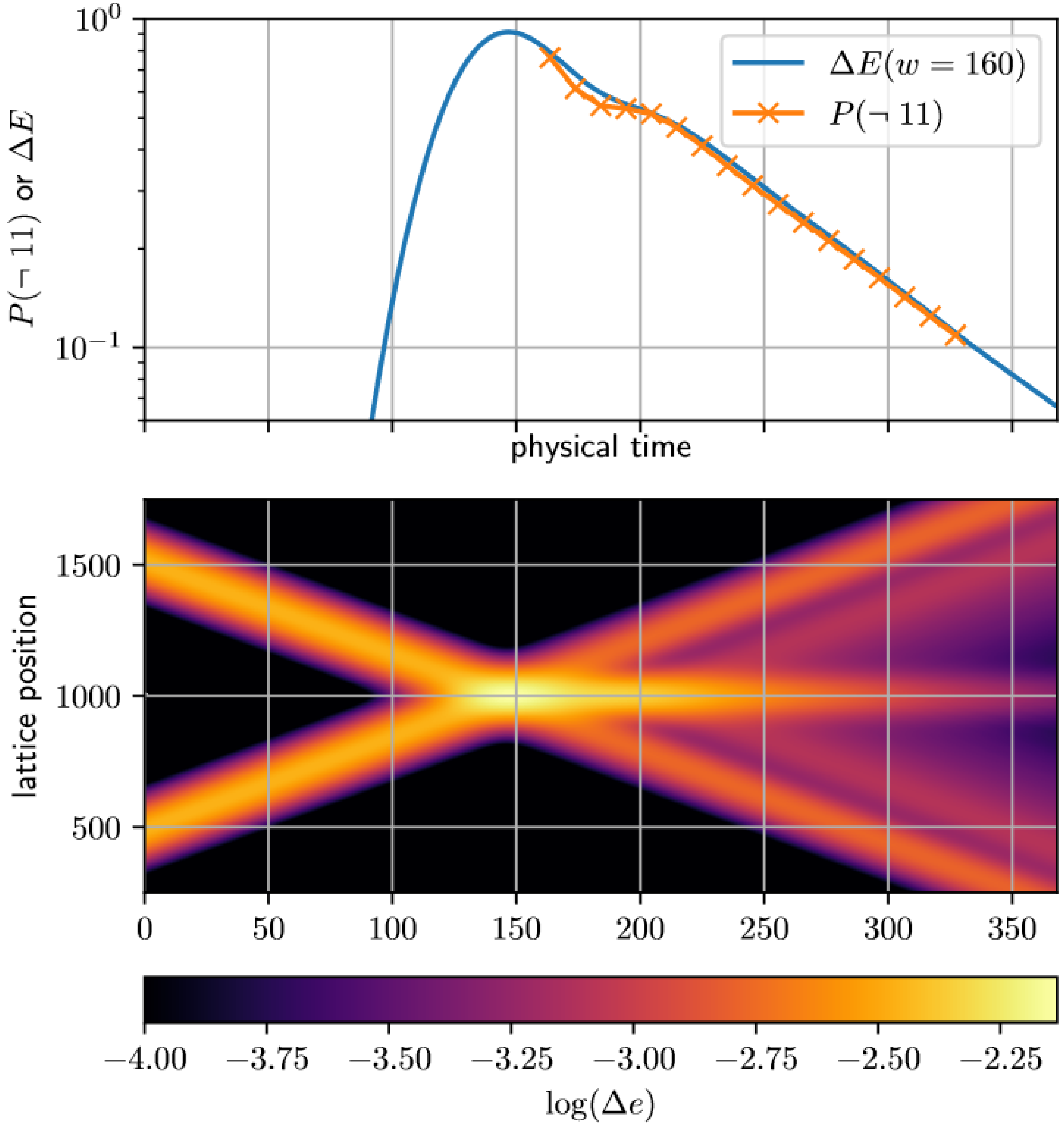

Resonance mass and width in the nonperturbative regime

TFFSA = truncated free-fermion space approach (Gabai and Yin 2022).

Further from E_8, our method may become less reliable.

“Leakage” into 12 and 21 sectors reduces the window in which resonance decay dominates.

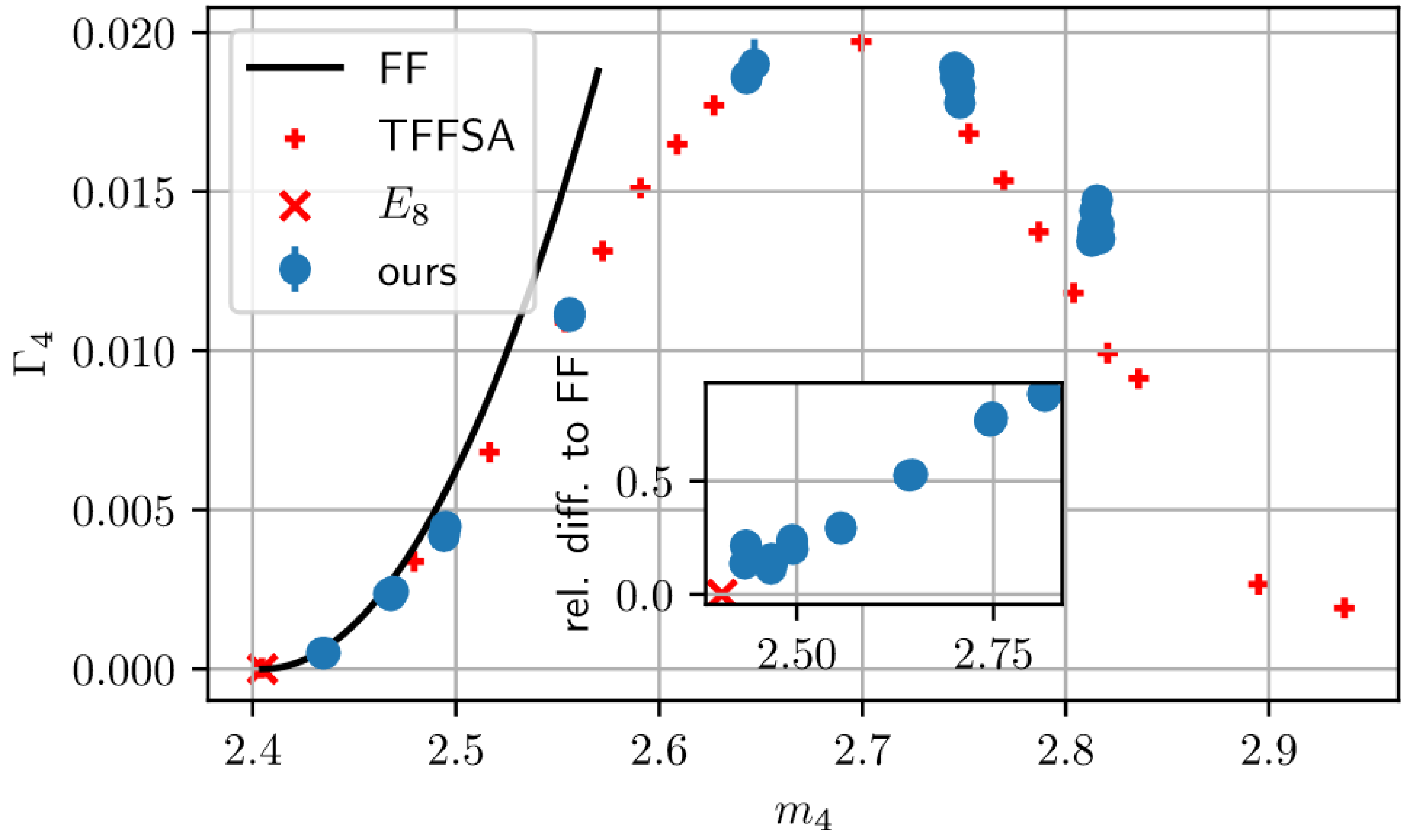

“Asymptotic” high-energy behavior of elastic scattering probability

Close to free fermions: *inelastic scattering becomes more probable* as energy increases.

Close to E_8: *elastic scattering becomes more probable* as energy increases.

Anticipated by Zamolodchikov 2013.

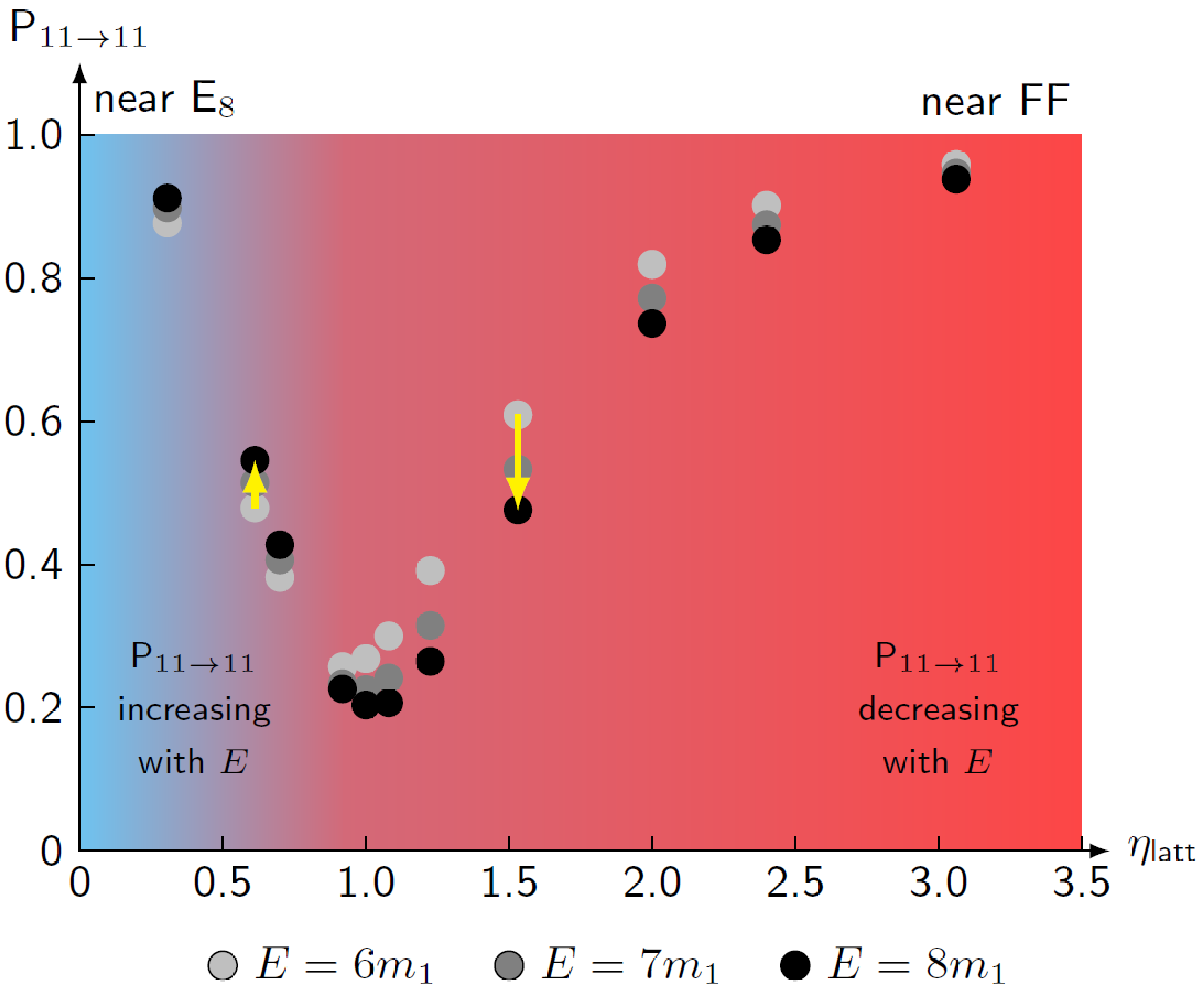

Real-time scattering in a strongly coupled nonintegrable QFT.

Final state channels appear in superposition. Project outgoing states onto particle sectors to compute branching fractions. Correlation functions clarify structure of outgoing states.

Observe time delay in elastic scattering to infer energy dependence of phase shifts.

Near integrable theories, compare with form-factor perturbation theory predictions. In strongly coupled regime, no previous predictions provide a basis for comparison.

Extract masses and widths of resonances.

Probability of elastic scattering at high energy.

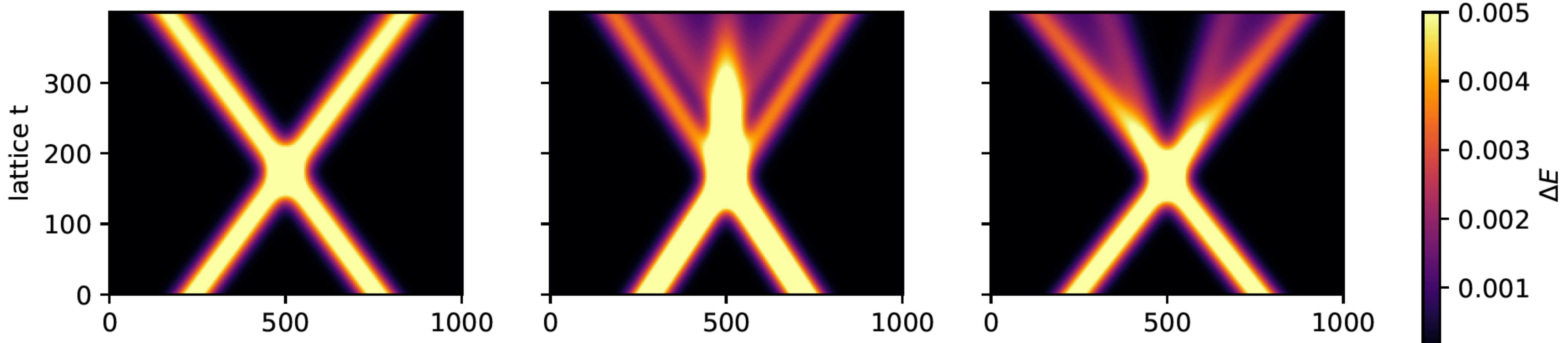

arXiv:2411.13645

Real-time scattering in a strongly coupled nonintegrable QFT.

More computation resources, better algorithms.

Higher energies, other resonances.

Other (1+1)-dimensional models: e.g., O(3), ϕ^4, Potts model, Schwinger model, …

Higher dimensions.

Input for bootstrap.

Quantum computers, perhaps in the “early fault-tolerant era.”